*Commemorating the 80th anniversary of Professor S.P. Gabuda*

# HIGH-FIELD SOLID-STATE $^{35}$Cl NMR IN SELENIUM(IV) AND TELLURIUM(IV) HEXACHLORIDES

## V.V. Terskikh[1], S. Pawsey[2], J.A. Ripmeester[3]

[1]*Department of Chemistry, University of Ottawa, 10 Marie Curie, Ottawa, Ontario K1N 6N5, Canada*
 E-mail: Victor.Terskikh@gmail.com
[2]*Bruker BioSpin Corporation, 15 Fortune Drive, Billerica, MA 01821, USA*
[3]*National Research Council Canada, 100 Sussex Drive, Ottawa, Ontario K1A 0R6, Canada*

We report solid-state $^{35}$Cl NMR spectra in three hexachlorides, $(NH_4)_2SeCl_6$, $(NH_4)_2TeCl_6$ and $Rb_2TeCl_6$. The $C_Q(^{35}Cl)$ quadrupole coupling constants in the three compounds were found to be 41.4±0.1 MHz, 30.3±0.1 MHz and 30.3±0.1 MHz, respectively, some of the largest $C_Q(^{35}Cl)$ quadrupole coupling constants ever measured in polycrystalline powdered solids directly via $^{35}$Cl NMR spectroscopy. The $^{35}$Cl EFG tensors are axial in all three cases reflecting the $C_{4v}$ point group symmetry of the chlorine sites. $^{35}$Cl NMR experiments in these compounds were only made possible by employing the WURST-QCPMG pulse sequence in the ultrahigh magnetic field of 21.1 T. $^{35}$Cl NMR results agree with the earlier reported $^{35}$Cl NQR values and with the complementary plane-wave DFT calculations. The origin of the very large $C_Q(^{35}Cl)$ quadrupole coupling constants in these and other main-group chlorides lies in the covalent-type chlorine bonding. The ionic bonding in the ionic chlorides results in significantly reduced $C_Q(^{35}Cl)$ values as illustrated with triphenyltellurium chloride $Ph_3TeCl$. The high sensitivity of $^{35}$Cl NMR to the chlorine coordination environment is demonstrated using tetrachlorohydroxotellurate hydrate $K[TeCl_4(OH)]\cdot0.5H_2O$ as an example. $^{125}$Te MAS NMR experiments were performed for tellurium compounds to support $^{35}$Cl NMR findings.

### INTRODUCTION

Despite its obvious attractiveness $^{35}$Cl NMR in solid state remains elusive owing to the ″difficult″ NMR properties of the $^{35}$Cl nuclide (Table 1) [1, 2]. The low resonance frequency coupled with a sizable quadrupole moment make $^{35}$Cl NMR challenging, at times even in fairly symmetric environments. The same is to be said about its less often studied sister nuclide $^{37}$Cl, which suffers from an

T a b l e   1

*NMR properties of $^{35}$Cl and $^{37}$Cl isotopes* [1]

| Nucleus | $I$ | N.A. % | $\nu_0$ (MHz) at 21.1 T | Quadrupole moment (mb) [2] | Sternheimer antishielding factor ($\gamma$) |
|---------|-----|--------|-------------------------|----------------------------|---------------------------------------------|
| $^{35}$Cl | 3/2 | 75.77 | 88.2 | −81.65 | −42.0 |
| $^{37}$Cl | 3/2 | 24.23 | 73.4 | −64.35 | −42.0 |

even lower resonance frequency and lower natural abundance, albeit it has a somewhat smaller quadrupole moment. Both chlorine isotopes are true low-gamma nuclei and have one of the largest Sternheimer antishielding factors in the periodic table. In practice, with the exception of the rare high symmetry cases, this result in extremely broad solid-state $^{35}$Cl NMR spectra dominated by strong quadrupolar coupling interactions and often spanning hundreds of kilohertz. Until recently solid-state $^{35}$Cl resonance studies remained in the domain of pure nuclear quadrupole resonance (NQR), where the NQR-measured $^{35}$Cl quadrupole coupling frequencies $\nu_{NQR}(^{35}$Cl) on the order of 20—40 MHz are typical [3]. Recent applications of $^{35}$Cl NQR, and NQR in general, range from structural and coordination chemistry [4] to explosives detection [5]. Gabuda and coworkers applied $^{35}$Cl NQR to study the channel inclusion compounds (clathrates) of thiourea with hexachloroethane [6]. CCl$_3$X guest molecules in hexakis(phenylthio)benzene clathrates were also studied by $^{35}$Cl NQR in [7]. While examples of $^{35}$Cl NQR are abundant, $^{35}$Cl NMR remains much less explored. Only with the advent and greater availability of high-field NMR instrumentation is $^{35}$Cl NMR in the solid-state gradually becoming more mainstream.

Several excellent recent review articles summarize the current state-of-the-art of the solid-state $^{35}$Cl and $^{37}$Cl NMR spectroscopy [8—11]. Pertinent to the research presented here, we will briefly mention some of the most important areas of ongoing development, both on the instrumentation side and on the application side. While the higher magnetic fields benefit NMR in general, it has been found particularly advantageous for solid-state applications when dealing with quadrupolar nuclei. Because the breadth of the EFG-dominated powder patterns will scale inversely with the magnetic field $B_0$, the higher magnetic field results in progressively narrower powder patterns thus making acquisition of such spectra more straightforward. Another limiting factor, the narrow excitation bandwidth of the square radiofrequency pulses, was recently circumvented by the introduction of WURST (Wideband Uniform Rate Smooth Truncation) pulses, which were found to be extremely helpful in recording ultra-wideline NMR spectra of not only quadrupolar but also spin-1/2 nuclei [12—15].

With respect to solid-state $^{35,37}$Cl NMR, the two opposite trends have been indentified in the recent literature. In ionic and mostly organic salts, i.e. hydrochlorides in particular, $C_Q(^{35}$Cl) quadrupole couplings are found in a convenient range of below 10 MHz, which allows for reasonably straightforward recording of the spectral data and its subsequent analysis [16—19]. In sufficiently high magnetic fields even magic-angle-spinning (MAS) $^{35,37}$Cl NMR is often possible with these samples. On the opposite end, the covalent and coordinate-covalent chlorides tend to have extremely large $^{35}$Cl quadrupole couplings, up to and in excess of 70 MHz, thus posing more severe experimental challenges for $^{35,37}$Cl NMR as compared to ionic salts, for example the quadrupole coupling constants $C_Q(^{35}$Cl) were found from 25 to 40 MHz in the group 13 metal chlorides [20]. In several transition metal organometallic complexes containing chlorine ligands the $^{35}$Cl EFG tensor parameters measured via $^{35}$Cl NMR were found to be sensitive to the chlorine bonding environment [21—23], which allowed the differentiation between bridging, terminal-axial and terminal-equatorial chlorine sites. The quadrupole coupling constants $C_Q(^{35}$Cl) were reported in the range from 15 to 40 MHz. In a related study [24] a series of platinum chloride complexes was investigated, and a $C_Q(^{35}$Cl) = 35.7 MHz was measured in K$_2$PtCl$_4$, with chlorine having close to an axial symmetry environment in the square-planar [PtCl$_4$]$^{2-}$ anion, $\eta_Q(^{35}$Cl) = 0.09.

The available $^{35}$Cl NMR information for the covalently-bonded main-group chlorides is very limited. In one such study $^{35}$Cl NMR spectra were recorded for a number of organo-germanates [25], and the $^{35}$Cl quadrupole coupling constants were reported to be from 14 to 43 MHz, depending on the germanium oxidation state. The tour-de-force solid-state $^{35,37}$Cl NMR study of covalent organic chlorides, the first study of its kind, was published very recently [26]. $^{35}$Cl and $^{37}$Cl NMR spectra recorded for several solid organic chlorides with the use of the WURST-QCPMG pulse sequence were in excess of 6—7 MHz broad, which is quite remarkable even at 21.1 T. Such strong $^{35,37}$Cl EFG interactions necessitated the exact treatment of the Zeeman-quadrupolar (ZQ) interaction in modeling the experimental spectra, since the second-order perturbation theory was no longer valid [27]. The $C_Q(^{35}$Cl) values were measured from 66 to 75 MHz for chlorine involved in the covalent C—Cl bonding, and reported to be sensitive to the carbon hybridization state.

The purpose of this work is to expand the range of the main-group covalent chlorides studied via [35]Cl NMR by including several selenium(IV) and tellurium(IV) chlorides. Experimental [35]Cl NMR results will be compared with the earlier NQR studies, and will be complemented by comprehensive *ab initio* DFT quantum chemistry calculations based on the reported crystal structures and using the CASTEP NMR software.

## MATERIALS AND METHODS

NMR experiments were performed with the following compounds, $(NH_4)_2SeCl_6$, $(NH_4)_2TeCl_6$, $Rb_2TeCl_6$, $Ph_3TeCl$, and $K[TeCl_4(OH)] \cdot 0.5H_2O$. The selenium and tellurium hexachlorides were prepared as described elsewhere [28] from the corresponding aqueous hydrochloric acid solutions. Triphenyltellurium chloride, $Ph_3TeCl$, was purchased from Organometallics Inc. (USA) and was used as received. The synthesis of $K[TeCl_4(OH)] \cdot 0.5H_2O$ is described in [29].

[35]Cl NMR experiments were performed with stationary powdered samples on a Bruker Avance II NMR spectrometer operating at 88.2 MHz (21.1 T) at the Canadian National Ultrahigh-Field NMR Facility for Solids (Ottawa, Canada). A home-built 4 mm double resonance H/X wideline solenoid probe with a two-coil design was used to perform all experiments. The samples were packed in 4 mm o.d. $ZrO_2$ MAS rotors. An aqueous solution of KCl (1M) was referenced at 0 ppm and was used to calibrate r.f. pulses, the liquid 90° pulse was set at 7 us. The WURST (Wideband Uniform Rate Smooth Truncation) modification of the QCMPG (Quadrupolar Carr-Purcell Meiboom-Gill) pulse se-

quence [14, 15] was used to acquire wideline [35]Cl NMR spectra in a frequency-offset manner. 50 us long WURST-80 pulses (2 MHz bandwidth) were used at 20 kHz r.f. power and were swept in one direction, the spikelet separation was 5 kHz. The WURST pulse power was adjusted to maximize the signal intensity. Inverting the sweep direction did not alter the spectra. The number of echoes in the echo train was typically 96 to 128. The relaxation delay was 1 s which was found sufficient for complete relaxation. For each O1 frequency step shifted by 500 kHz from 128 to 256 scans were acquired. The spectral sweep-width was 4 MHz. Proton decoupling at 25 kHz was used when needed, for example in ammonium salts and in organics, to allow for more echoes to be acquired in the FID due to longer $T_2$ relaxation times when decoupling was applied. The individual stepped-frequency spectra acquired for each sample were co-added using the sky-line projection method in order to obtain the profile of the entire spectrum. As a typical example, the entire [35]Cl WURST-QCPMG NMR spectrum in $Rb_2TeCl_6$ (Fig. 1) was recorded using three O1 steps separated by 500 kHz, each was recorded using 128 scans
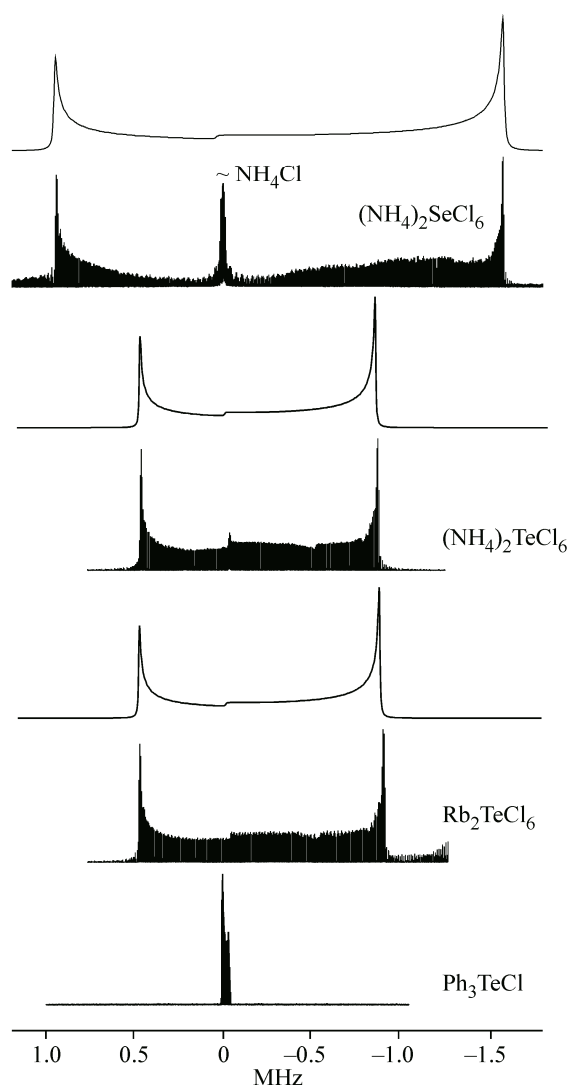


*Fig. 1.* Experimental (below) and simulated (above) [35]Cl WURST-QCPMG NMR spectra in powdered stationary samples of $(NH_4)_2SeCl_6$, $(NH_4)_2TeCl_6$, $Rb_2TeCl_6$ and $Ph_3TeCl$ acquired at 21.1 T. In $(NH_4)_2SeCl_6$ the strong narrow signal at about 0 ppm from $NH_4Cl$ impurity was truncated for clarity. See Table 2 for the parameters used in simulations

and 1 s relaxation delay, with the total experimental time needed to acquire the complete spectrum in just over 6 min. This compares favourably with about 20 h of acquisition needed to acquire a similar-quality spectrum when using the standard QCPMG pulse sequence. In the latter the square 180 pulses which are used to propagate the QCPMG echo train severely limit the excitation bandwidth thus requiring many more frequency offset steps to be completed.

$^{125}$Te NMR experiments were performed at 284.0 MHz (21.1 T) under MAS conditions (16 kHz) using a 4 mm H/X MAS Bruker probe. A single short r.f. pulse of 2 us (pi/4) was used with a relaxation delay of 30 s, and the number of scans from 128 to 2048. The spectra were referenced to external Te(CH$_3$)$_2$ at 0 ppm using solid telluric acid Te(OH)$_6$ (10 kHz MAS) as a secondary chemical shift reference (two resonances at +692.2 and +685.5 ppm) [30].

All experimental $^{35}$Cl NMR spectra were simulated using DMFit software [31] to extract the quadrupole coupling constant $C_Q(^{35}Cl)$, the EFG tensor asymmetry parameter $\eta_Q(^{35}Cl)$, and the isotropic chemical shift $\delta_{iso}(^{35}Cl)$. The quadrupole coupling parameters were then compared to the literature values as available from reported NQR experiments. CASTEP NMR calculations indicated the likely presence of small $^{35}$Cl chemical shielding anisotropies in all three hexachlorides (about 200—300 ppm, see text), however none was included in the spectral simulations due to its negligible contribution to the overall spectral lineshape.

*Ab initio* plane-wave density functional theory (DFT) calculations of the nuclear magnetic resonance parameters were performed using the CASTEP NMR program [32, 33] in the Materials Studio 4.4 environment (Accelrys) running on a HP xw4400 workstation with a single Intel dual-core 2.67 GHz processor and 8 GB DDR RAM. Ultrasoft pseudopotentials were used for $^{35}$Cl EFG calculations with plane wave basis set energy cut-off of 400 eV in a fine accuracy basis set with the Monkhorst-Pack k-space grid size of (2×2×2). The Perdew, Burke and Ernzerhof (PBE) functionals were used in the generalized gradient approximation (GGA) for the exchange-correlation energy. The nuclear quadruple moment for $^{35}$Cl was corrected to be –81.65 Mb to reflect the most recently tabulated value [2]. The magnetic shielding tensors for $^{35}$Cl were calculated in a medium accuracy basis set using the projector augmented-wave method (GIPAW) implemented in the CASTEP code [34, 35]. The crystal structures used in the calculations were built using atomic coordinates from available X-ray diffraction data as indicated (Table 1). In the crystal structures for ammonium salts missing protons of NH$_4^+$ cations were added at assumed positions and the full geometry optimization was performed while constraining the unit cell parameters. The full geometry optimization was also performed for Ph$_3$TeCl. Due to the very large unit cell size in the latter compound only $^{35}$Cl EFG parameters were calculated in the coarse accuracy basis set and using the plane wave basis set cut-off of 200 eV, and the k-space grid size of (1×1×1). The isotropic chemical shifts, $\delta_{iso}(^{35}Cl)$, were re-calculated from the isotropic shieldings, $\sigma_{iso}(^{35}Cl)$, as $\delta_{iso}(^{35}Cl) \approx \sigma_{ref}(^{35}Cl) - \sigma_{iso}(^{35}Cl)$, where $\sigma_{ref}(^{35}Cl)$ is the shielding of the known solid reference sample calculated using the same conditions, $\sigma_{ref}(^{35}Cl, NaCl_{solid}) = 996.2$ ppm.

## RESULTS AND DISCUSSIONS

**Covalent selenium(IV) and tellurium(IV) hexachlorides.** Three selenium(IV) and tellurium(IV) hexachlorides studied in this work, (NH$_4$)$_2$SeCl$_6$, (NH$_4$)$_2$TeCl$_6$ and Rb$_2$TeCl$_6$, belong to the cubic *Fm*-3*m* space group of the K$_2$PtCl$_6$ structure type [36—39]. The crystal structure is composed of the isolated [SeCl$_6$]$^{2-}$ and [TeCl$_6$]$^{2-}$ octahedra belonging to the $O_h$ point group symmetry. The Se—Cl bond distance in [SeCl$_6$]$^{2-}$ is 2.384 Å, and the Te—Cl bond distance is 2.507 Å in Rb$_2$TeCl$_6$, and 2.545 Å in (NH$_4$)$_2$TeCl$_6$ indicating covalent bonding. Both types of hexachlorides, [SeCl$_6$]$^{2-}$ and [TeCl$_6$]$^{2-}$, are the classic examples of complexes with the stereochemically inactive lone pair. While the electronic configuration in both is the 14-electron MX$_6$E type (E — the lone pair), the lone electron pair resides in the corresponding stereochemically inactive *n*s orbitals. This results in regular octahedral coordination of [SeCl$_6$]$^{2-}$ and [TeCl$_6$]$^{2-}$ found in a large number of selenium and tellurium chloride compounds [40]. Gabuda and coworkers studied effects of the lone electron pair on $^{125}$Te NMR spectra and the electronic structure in solid paratellurite TeO$_2$ and in several other related systems [41—44].

*Experimental and calculated* $^{35}$Cl NMR *parameters in studied compounds*

| Compound | Technique | Structure | $\lvert C_Q \rvert$, MHz $\pm 0.1$ | $\eta_Q$ $\pm 0.02$ | $\delta_{iso}$, ppm $\pm 50$ |
|---|---|---|---|---|---|
| $(NH_4)_2SeCl_6$ | NMR | | 41.4 | 0.00 | 490 |
| | NQR [3] | | 41.4 | | |
| | CASTEP | *Fm*-3*m* [ 36 ] | 40.5 | 0.00 | 487 |
| $(NH_4)_2TeCl_6$ | NMR | | 30.3 | 0.00 | 280 |
| | NQR [3] | | 30.3 | | |
| | CASTEP | *Fm*-3*m* [ 36 ] | 30.5 | 0.00 | 348 |
| $Rb_2TeCl_6$ | NMR | | 30.3 | 0.00 | 260 |
| | NQR [3] | | 30.3 | | |
| | CASTEP | *Fm*-3*m* [ 36 ] | 31.8 | 0.00 | 369 |
| $K_2TeCl_6$ | CASTEP | *I*12/*m*1 [ 36 ] | (×2) 31.6 | 0.00 | 372 |
| | | | (×4) 33.1 | 0.02 | 413 |
| $K[TeCl_4(OH)]\cdot 0.5H_2O$ | NMR | | 33.2 | 0.17 | 410 |
| | CASTEP | *P*2$_1$/*c* [ 29 ] | 31.6 | 0.18 | 417 |
| | | | 35.4 | 0.15 | 418 |
| | | | 30.2 | 0.07 | 397 |
| | | | 32.5 | 0.10 | 413 |
| $Ph_3TeCl$ | NMR | | 5.1 | 0.20 | 180 |
| | CASTEP | *P*2$_1$/*c* [ 52, 53 ] | (×1) 7.7 | 0.15 | |
| | | | (×1) 8.1 | 0.14 | |

In all three hexachloride crystal structures there is only one unique Cl site residing on the octahedron vertices. The point group symmetry of the chlorine site is $C_{4v}$ which implies the high axially symmetric $^{35}$Cl EFG tensor, with the largest component $V_{zz}$ along the M—Cl bond. The corresponding solid-state $^{35}$Cl NMR spectra recorded for three hexachlorides at 21.1 T are shown in Fig. 1. The lineshapes are typical of the axially symmetric cases, $\eta_Q(^{35}\text{Cl}) = 0.00$. The full breadth of each spectrum is remarkable, and is about 2.5 MHz in $(NH_4)_2SeCl_6$, and is somewhat narrower in $(NH_4)_2TeCl_6$ and $Rb_2TeCl_6$, at about 1.5 MHz. The spectral simulations produced the $C_Q(^{35}\text{Cl})$ quadrupole coupling constants of 41.4±0.1 MHz, 30.3±0.1 MHz and 30.3±0.1 MHz, in the three compounds respectively (Table 2). The isotropic chemical shift $\delta_{iso}(^{35}\text{Cl})$ is about +500 ppm in the selenium chloride, and is about +300 ppm in the two tellurium chlorides. The $^{35}$Cl isotropic chemical shifts are listed with significant uncertainty ±50 ppm due to the very broad powder patterns and the nature of the WURST-QCPMG pulse sequence. Because the spikelet separation was 5 kHz (see Experimental, 5 kHz equals 57 ppm at 88.2 MHz, the resonance frequency of $^{35}$Cl at 21.1 T), in these experiments the $^{35}$Cl chemical shifts cannot be determined with higher accuracy. Nevertheless, the difference in the isotropic chemical shifts $\delta_{iso}(^{35}\text{Cl})$ determined for $[SeCl_6]^{2-}$ and $[TeCl_6]^{2-}$ is beyond this experimental uncertainty and is supported by CASTEP calculations.

CASTEP computed values for the $^{35}$Cl EFG tensor parameters in three hexachlorides based on the reported crystal structures are in very good agreement with the experimental results (Table 2). All CASTEP calculated $C_Q(^{35}\text{Cl})$ values were negative as was also found in other terminal covalent chlorine sites [ 21 ]. As was mentioned above, a small $^{35}$Cl CSA anisotropy of about 200—300 ppm is predicted in these compounds by CASTEP (axial CSA tensor, coincident with the EFG tensor and is along the M—Cl bond). This anisotropy is negligible against the EFG dominated powder patterns which are about 20000 ppm broad, and it was not taken into account while modeling the spectra shown in Fig. 1.
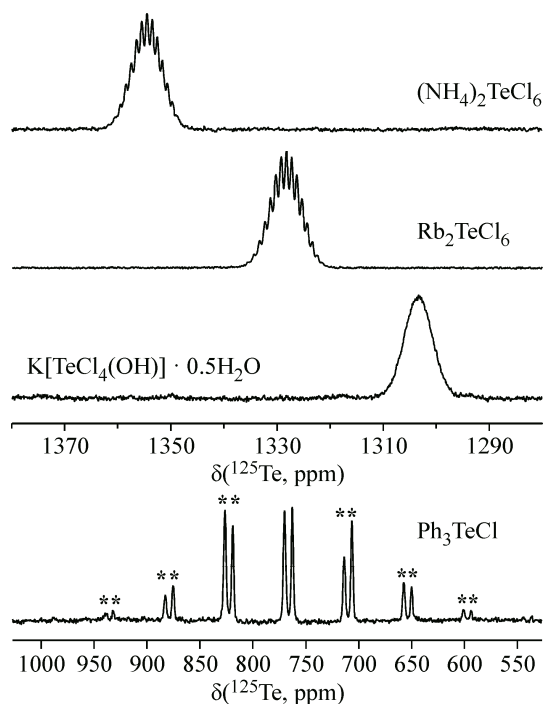
*Fig. 2.* $^{125}$Te MAS NMR spectra in four tellurium chloride compounds recorded at 21.1 T and 16 kHz MAS. The characteristic multiplet splitting patter observed in $(NH_4)_2TeCl_6$ ($\delta_{iso}$ = 1353.5 ppm) and $Rb_2TeCl_6$ ($\delta_{iso}$ = 1327.1 ppm) is due to $^1J(^{125}Te—^{35,37}Cl)$ = 280 Hz coupling. Note that in $K[TeCl_4(OH)]\cdot 0.5H_2O$ ($\delta_{iso}$ = 1302.2 ppm) the splitting is getting smeared while the total linewidth remaining the same, most likely due overlap from multiple non-equivalent Cl sites in the crystal structure (see text). The spectrum in $Ph_3TeCl$ indicates two non-equivalent $Ph_3Te^+$ cations in the asymmetric unit, the isotropic resonances are at +763.8 and +771.1 ppm, note the absence of $^1J(^{125}Te—^{35,37}Cl)$ splitting in this case. (*) indicates MAS spinning sidebands

The $C_Q(^{35}Cl)$ quadrupole coupling constants in all three compounds are well known from the previous $^{35}$Cl NQR experiments [3], and are identical to the values measured in this work via $^{35}$Cl NMR (Table 2). We note, however, that in the powdered polycrystalline samples only the NQR frequency $\nu_{NQR}(^{35}Cl)$ can be measured by $^{35}$Cl NQR, $^{35}$Cl being spin-3/2. The relationship between the two depends on the asymmetry of the EFG tensor, $\nu_{NQR} = (C_Q/2)(1 + \eta_Q^2/3)^{1/2}$. While in the studied hexachlorides the EFG tensor symmetry is constrained by the point group symmetry of the chlorine site ($\eta_Q$ = 0.0) resulting in $\nu_{NQR} = C_Q/2$, this however cannot be generalized to the cases of lower symmetry as will be shown below.

The quadrupole coupling constant $C_Q(^{35}Cl)$ = 41.4 MHz found in $[SeCl_6]^{2-}$ is notably larger compared with 30.3 MHz measured in the two $[TeCl_6]^{2-}$ salts, the fact which was attributed to the higher electronegativity of selenium leading to the greater covalent character of Se—Cl bonds comparing with Te—Cl bonds [45, 46]. In the same report $C_Q(^{35}Cl)$ values in isostructural selenium and tellurium hexachlorides were found to be virtually independent on the nature of the counter cation, $NH_4^+$, $K^+$, $Rb^+$ etc, in agreement with the present NMR study.

$^{125}$Te MAS NMR spectra acquired for $(NH_4)_2TeCl_6$ and $Rb_2TeCl_6$ (Fig. 2) confirm single Te site in each compound. The isotropic chemical shift values, $\delta_{iso}(^{125}Te)$ = 1353.5 ppm in $(NH_4)_2TeCl_6$ and $\delta_{iso}(^{125}Te)$ = 1327.1 ppm in $Rb_2TeCl_6$, are similar to those reported for the $[TeCl_6]^{2-}$ anion in the liquid state, for example +1531.7 ppm in the $(Et_2NH_2)_2[TeCl_6]$ solution in DMSO [47], +1548 ppm in the tetrahydrofuran solution of $[(Me_2SO)_2H]_2[TeCl_6]$ [48], and +1469 ppm in the acetonitrile solution of $(Ph_3Te)_2[TeCl_6]$ [49].

The prominent feature in the $^{125}$Te MAS NMR spectra of the two tellurium hexachlorides is the characteristic multiplet splitting pattern originating from indirect spin coupling between tellurium and six equivalent Cl atoms, $^1J(^{125}Te—^{35,37}Cl)$ = 280 Hz. Similar splitting was reported previously in $^{125}$Te MAS NMR spectra of other tellurium chlorides, for example $^1J(^{125}Te—^{35,37}Cl)$ = 106 Hz was found in $(CH_3)_3TeCl\cdot H_2O$ [30], and $^1J(^{125}Te—^{35,37}Cl)$ = 65 Hz was estimated in anhydrous $(CH_3)_3TeCl$ [50]. Likewise, $^1J(^{195}Pt—^{35,37}Cl)$ from 138 to 145 Hz was found in $^{195}$Pt MAS NMR spectra recorded for $(NH_4)_2PtCl_6$ and several alkali metal hexachloroplatinates(IV) [51].

**Ionic chloride Ph$_3$TeCl.** Triphenyltellurium chloride $Ph_3TeCl$ crystallizes in the monoclinic space group $P2_1/c$ [52, 53]. The asymmetric unit contains two non-equivalent $Ph_3TeCl$ molecules. The Te—Cl distance is long at 3.204 Å (averaged over four Te—Cl bonds), and the compound is con-

sidered predominantly ionic in the solid state, two $Ph_3Te^+$ ions form a dimer bridged by two $Cl^-$ cations. The ionic character of crystal bonding in $Ph_3TeCl$ results in dramatically different $^{35}Cl$ NMR spectra when compared with covalent chlorides (Fig. 1). The total static spectral width is now only about 50 kHz (at 21.1 T), so that not only traditional spin-echo experiments were possible in the stationary sample, but also $^{35}Cl$ MAS NMR was done under moderate spinning speed of 20 kHz (spectra not shown). While there are two $Cl^-$ ions in the asymmetric unit, only one average signal was resolved in $^{35}Cl$ MAS NMR spectra, $C_Q(^{35}Cl) = 5.10$ MHz, $\eta_Q(^{35}Cl) = 0.20$, in good agreement with the CASTEP computed EFG values (Table 2). $Ph_3TeCl$ was the only compound studied in this work where CASTEP predicted a positive value for $C_Q(^{35}Cl)$, this is in contrast with negative $C_Q(^{35}Cl)$'s calculated in all other Se and Te chlorides where chlorine is found in the terminal covalent bonding environment.

The $^{35}Cl$ chemical shielding anisotropy was apparent in the stationary $^{35}Cl$ NMR spectra recorded for $Ph_3TeCl$, $\delta_{iso}(^{35}Cl) = 180$ ppm, $\Delta\delta = 75$ ppm, $\eta\delta = 0.1$. There are no high symmetry elements associated with the chlorine sites, and the EFG and CSA tensors were found non-coincident, the Euler angles were determined as $\alpha = 45°$, $\beta = 30°$, $\gamma = 10°$. The $^{35}Cl$ NMR parameters found in $Ph_3TeCl$ resemble those measured in other ionic organic chlorides [16—19]. We note, that while the $C_Q(^{35}Cl)$ value found in $Ph_3TeCl$ (5.1 MHz) is only about six times smaller comparing with $(NH_4)_2TeCl_6$ and $Rb_2TeCl_6$ (30.3 MHz), the spectral breadth is about 36 times smaller because of the squared dependence on $C_Q$.

$^{125}Te$ MAS NMR spectra in $Ph_3TeCl$ consist of two sharp resonances (1:1), at +763.8 ppm and +771.1 ppm, consistent with two non-equivalent $Ph_3TeCl$ molecules in the asymmetric unit. $^{125}Te$ NMR chemical shift for $Ph_3Te^+$ ions in solutions was reported at +754 ppm in nitric acid and at +788 ppm in ethanol [54]. In agreement with the ionic nature of $Ph_3TeCl$, the indirect $^1J(^{125}Te-^{35,37}Cl)$ coupling was not observed.

In a related compound, bis(triphenyltelluronium)hexachlorotellurate $(Ph_3Te)_2[TeCl_6]$, two separate $^{125}Te$ NMR signals were observed in the acetonitrile solution [49], at +757 ppm from $Ph_3Te^+$ cations, and at +1469 ppm from $[TeCl_6]^{2-}$ anions. In the crystal structure the two ions are linked by the weak $Te\cdots Cl$ secondary bonds of 3.527 Å, while the $[TeCl_6]^{2-}$ tellurate ion is an almost ideal octahedron, resembling the tellurium hexachlorides discussed above.

**Case study, tetrachlorohydroxotellurate $K[TeCl_4(OH)]\cdot 0.5H_2O$.** We will start by discussing the crystal structure of the related compound, potassium hexachlorotellurate $K_2TeCl_6$. Although $^{35}Cl$ NMR spectra for this compound were not recorded in the current study, CASTEP computations predict spectra similar to the spectra recorded for selenium(IV) and tellurium(IV) hexachlorides as shown in Fig. 1. $K_2TeCl_6$ crystallizes in the monoclinic $I12m/1$ space group [36], the $[TeCl_6]^{2-}$ octahedron is slightly distorted axially, the equatorial $Te-Cl_2$ bond distances (×4) are 2.545 Å, and the two axial $Cl_1$ atoms are at 2.535 Å. This geometry suggests two overlapping powder patterns in the $^{35}Cl$ NMR spectrum, the two $Cl_1$ sites will have high axial EFG symmetry, $\eta_Q(^{35}Cl) = 0.00$ ($C_4$ point group symmetry), and the four equatorial $Cl_2$ sites will be slightly off-axial, $\eta_Q(^{35}Cl) = 0.02$, reflecting the lower $C_2$ point group symmetry. The $^{35}Cl$ quadrupole coupling constants for chlorine sites in $K_2TeCl_6$ are predicted to be in the same range as for other covalent hexachlorotellurates, $C_Q(^{35}Cl) = 31.6$ MHz ($Cl_1$) and $C_Q(^{35}Cl) = 33.1$ MHz ($Cl_2$) (Table 2, Fig. 3, **4**).

The title compound, tetrachlorohydroxotellurate semihydrate $K[TeCl_4(OH)]\cdot 0.5H_2O$, can be considered as the hydrolysis product of $K_2TeCl_6$. The crystal structure was solved as monoclinic, space group $P2_1/c$ [29]. The unit cell contains two types of isolated and somewhat distorted square pyramidal $TeCl_4(OH)^-$ ions (OH axial), one of which is disordered over two sites. In the ordered $TeCl_4(OH)^-$ ion ($Te_2$), the $Te-Cl$ distances were found from 2.478 to 2.516 Å, similar to $[TeCl_6]^{2-}$ in hexachlorotellurates. The $O-Te-Cl$ angles in $TeCl_4(OH)^-$ range from 83.84° to 86.09°. This distorted geometry suggests four overlapping non-axial $^{35}Cl$ NMR powder patterns, as was also confirmed by CASTEP calculations (Table 2).

The experimental $^{35}Cl$ WURST-QCPMG NMR spectrum acquired for the powdered stationary $K[TeCl_4(OH)]\cdot 0.5H_2O$ sample is shown in Fig. 3, **1**. As with other covalent chlorides, this spectrum is

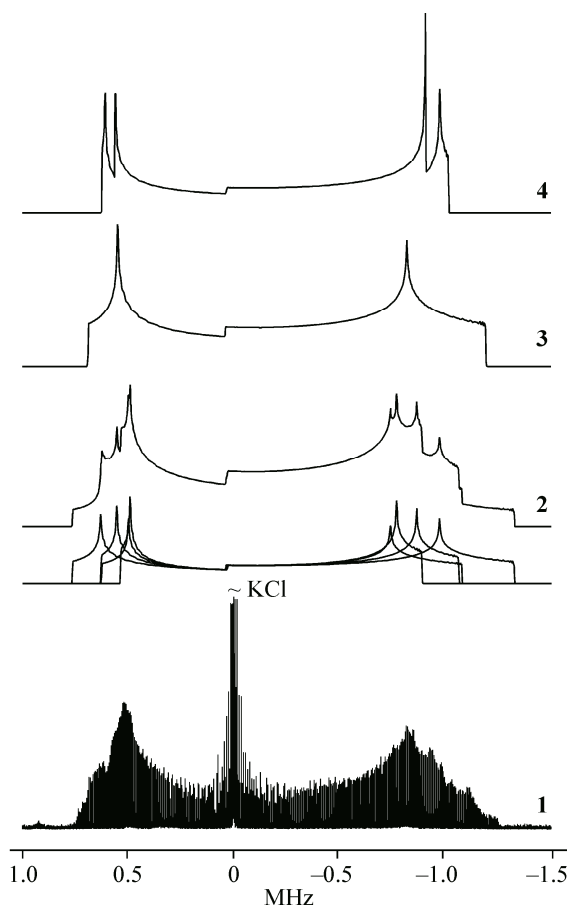*Fig. 3.* Experimental $^{35}$Cl WURST-QCPMG NMR spectrum in a powdered stationary sample of K[TeCl$_4$(OH)]·0.5H$_2$O at 21.1 T (**1**). The strong narrow signal at about 0 ppm from KCl impurity was truncated for clarity. Four-site model based on CASTEP calculations with four individual components shown below, see Table 2 for the simulation parameters (**2**). Single-site model using the following parameters, $C_Q = 33.2$ MHz, $\eta_Q = 0.17$, $\delta_{iso} = 410$ ppm (**3**). Two-site model predicted for K$_2$TeCl$_6$ (monoclinic) based on CASTEP (**4**)

extremely broad and covers over 2 MHz spectral width. There are clearly several overlapping patterns present. The striking difference of this spectrum when compared with the $^{35}$Cl NMR spectra recorded for Rb$_2$TeCl$_6$ and (NH$_4$)$_2$TeCl$_6$ (Fig. 1) and predicted for K$_2$TeCl$_6$ (Fig. 3, **4**) is significant non-axial symmetry of the corresponding $^{35}$Cl EFG tensors. While fitting of this spectrum by individual components will be highly ambiguous considering the disordered nature of the crystal structure, the average $^{35}$Cl NMR parameters can still be extracted, $C_Q(^{35}$Cl$) = 33.2$ MHz, $\eta_Q(^{35}$Cl$) = 0.17$, $\delta_{iso}(^{35}$Cl$) = 410$ ppm (Fig. 3, **3**, Table 2). CASTEP calculations were performed for the ordered TeCl$_4$(OH)$^-$ ion (Te$_2$), and the computed parameters were in good agreement with the experimental spectrum (Fig. 3, **2**). The $C_Q(^{35}$Cl$)$ in K[TeCl$_4$(OH)]·0.5H$_2$O is somewhat larger comparing with the other two covalent hexachlorotellurates studied in this work, most likely due to shorter Te—Cl bonds in the former. The non-axial EFG tensor, $\eta_Q(^{35}$Cl$) = 0.17$, reflects the low symmetry of the chlorine sites. The spectrum in Fig. 3, **1** resembles the $^{35}$Cl NMR spectrum reported recently for MoOCl$_4$ having a similar square pyramidal arrangement around Mo [21]. It is important to note here that it would be impossible to measure the $C_Q(^{35}$Cl$)$ quadrupole coupling constant accurately in this compound via $^{35}$Cl NQR because the $^{35}$Cl EFG tensor is non-axial. In polycrystalline powdered samples, $C_Q(^{35}$Cl$)$ and $\eta_Q(^{35}$Cl$)$, can only be measured simultaneously and with precision by using $^{35}$Cl NMR spectroscopy.

The anhydrous version of the title compound, K[TeCl$_4$(OH)], was suggested polymeric with chlorine bridging [29]. In such a case, the $C_Q(^{35}$Cl$)$ quadrupole coupling constant is expected to be significantly reduced to as low as 10—15 MHz, as was reported for a number of covalent transition-metal chlorides containing Cl bridging [21—23]. No bridging chlorides were detected in the $^{35}$Cl NMR spectra of the semihydrate (Fig. 3).

$^{125}$Te MAS NMR spectra recorded for K[TeCl$_4$(OH)]·0.5H$_2$O reflect the disordered nature of its crystal structure (Fig. 2). While the total linewidth is similar to that of the corresponding $^{125}$Te MAS NMR spectra in (NH$_4$)$_2$TeCl$_6$ and Rb$_2$TeCl$_6$, the splitting pattern due to indirect $^{125}$Te—$^{35,37}$Cl spin coupling is smeared owing to multiple non-equivalent chlorine sites present in the crystal structure.

To conclude this short case study exercise, we have shown that solid-state $^{35}$Cl NMR is capable of distinguishing among three related and chemically similar compounds containing covalently bound chlorine, K$_2$TeCl$_6$, K[TeCl$_4$(OH)]·0.5H$_2$O, and anhydrous K[TeCl$_4$(OH)]. We anticipate that $^{35}$Cl NMR will be able to aid in future structural studies and crystallographic assignments involving these and similar systems.

**CONCLUSIONS**

In this brief report we have presented the $^{35}$Cl quadrupole coupling parameters measured by solid-state $^{35}$Cl NMR in three cubic selenium(IV) and tellurium(IV) hexachlorides. The measured $C_Q(^{35}$Cl) values, 41.4 MHz in $(NH_4)_2SeCl_6$ and 30.3 MHz in $(NH_4)_2TeCl_6$ and in $Rb_2TeCl_6$, are among the largest $^{35}$Cl quadrupole coupling constants reported this far by NMR. The EFG tensors are axial in all three compounds, $\eta_Q(^{35}$Cl) = 0.0 reflecting the $C_{4v}$ point group symmetry of the chlorine site. The corresponding $^{35}$Cl NMR spectra at 21.1 T span from 1.5 MHz in $(NH_4)_2TeCl_6$ and $Rb_2TeCl_6$ to 2.5 MHz in $(NH_4)_2SeCl_6$ making the recording of these ultra-wide spectra of sufficient quality and in reasonable time only possible by employing the WURST-QCPMG pulse sequence. $^{35}$Cl NMR data agree with the earlier $^{35}$Cl NQR reports and with the complementary plane-wave DFT CASTEP calculations. Two additional examples of $^{35}$Cl NMR performed in ionic $Ph_3TeCl$ chloride and in tetrachlorohydroxotellurate semihydrate $K[TeCl_4(OH)]\cdot 0.5H_2O$ illustrate the great versatility of the $^{35}$Cl NMR technique and its high sensitivity to provide insight into a variety of chlorine environments in solid state phases. We hope that this work will contribute to the growing field of $^{35}$Cl NMR knowledge and will encourage further research in this area.

*REFERENCES*

1. *Mackenzie K.J.D., Smith M.E.* Multinuclear Solid-State NMR of Inorganic Materials. – Pergamon, 2002.
2. *Pyykkö P.* // Mol. Phys. – 2008. – **106**. – P. 1965.
3. *Semin G.K., Babushkina T.A., Yakobson G.G.* Nuclear Quadrupole Resonance in Chemistry. – New York: John Wiley & Sons, 1975.
4. *Buslaev Yu.A., Kravčenko E.A., Kolditz L.* // Coord. Chem. Rev. – 1987. – **82**. – P. 9.
5. *Explosives* Detection Using Magnetic and Nuclear Resonance Techniques / Eds. J. Fraissard, O. Lapina. – NATO Science for Peace and Security Series B: Physics and Biophysics. – Springer, 2009. – P. 1 – 292.
6. *Krieger Ju.H., Kozlova S.G., Gabuda S.P., Chehova G.N., Dyadin Yu.N.* // Sov. Phys. Solid State. – 1985. – **27**. – P. 1875. [Fiz. Tverd. Tela (Leningrad). – 1985. – **27**. – S. 3121.]
7. *Pang L., Brisse F., Lucken E.A.C.* // Can. J. Chem. – 1995. – **73**. – P. 351.
8. *Szell P.M.J., Bryce D.L.* // Ann. Rep. NMR Spectr. – 2015. – **84**. – P. 115.
9. *Bryce D.L., Widdifield C.M., Chapman R.P., Attrell R.J.* Chlorine, Bromine, and Iodine Solid-State NMR. Encyclopedia of Magnetic Resonance. – Wiley, 2011.
10. *Widdifield C.M., Chapman R.P., Bryce D.L.* // Ann. Rep. NMR Spectr. – 2009. – **66**. – P. 195.
11. *Chapman R.P., Widdifield C.M., Bryce D.L.* // Prog. Nucl. Magn. Res. Spectr. – 2009. – **55**. – P. 215.
12. *Schurko R.W.* // Acc. Chem. Res. – 2013. – **46**. – P.1985.
13. *Schurko R.W.* Acquisition of Wideline Solid-State NMR Spectra of Quadrupolar Nuclei. Encyclopedia of Magnetic Resonance. – Wiley, 2011.
14. *O'Dell L.A., Rossini A.J., Schurko R.W.* // Chem. Phys. Lett. – 2009. – **468**. – P. 330.
15. *O'Dell L.A., Schurko R.W.* // Chem. Phys. Lett. – 2008. – **464**. – P. 97.
16. *Hildebrand M.P., Hamaed H., Namespetra A.M., Donohue J.M., Fu R., Hung I., Gan Z., Schurko R.W.* // CrystEngComm. – 2014. – **16**. – P. 7334.
17. *Chapman R.P., Hiscock J.R., Gale P.A., Bryce D.L.* // Can. J. Chem. – 2011. – **89**. – P. 822.
18. *Hamaed H., Pawlowski J.M., Cooper B.F.T., Fu R., Eichhorn S.H., Schurko R.W.* // J. Am. Chem. Soc. – 2008. – **130**. – P. 11056.
19. *Chapman R.P., Bryce D.L.* // Phys. Chem. Chem. Phys. – 2007. – **9**. – P. 6219.
20. *Chapman R.P., Bryce D.L.* // Phys. Chem. Chem. Phys. – 2009. – **11**. – P. 6987.
21. *O'Keefe C.A., Johnston K.E., Sutter K., Autschbach J., Gauvin R., Trébosc J., Delevoye L., Popoff N., Taoufik M., Oudatchin K., Schurko R.W.* // Inorg. Chem. – 2014. – **53**. – P. 9581.

22. *Johnston K.E., O'Keefe C.A., Gauvin R.M., Trébosc J., Delevoye L., Amoureux J.-P., Popoff N., Taoufik M., Oudatchin K., Schurko R.W.* // Chem. Eur. J. – 2013. – **19**. – P. 12396.

23. *Rossini A.J., Mills R.W., Briscoe G.A., Norton E.L., Geier S.J., Hung I., Zheng S., Autschbach J., Schurko R.W.* // J. Am. Chem. Soc. – 2009. – **131**. – P. 3317.

24. *Lucier B.E.G., Johnston K.E., Xu W., Hanson J.C., Senanayake S.D., Yao S., Bourassa M.W., Srebro M., Autschbach J., Schurko R.W.* // J. Am. Chem. Soc. – 2014. – **136**. – P. 1333.

25. *Hanson M.A., Terskikh V.V., Baines K.M., Huang Y.* // Inorg. Chem. – 2014. – **53**. – P. 7377.

26. *Perras F.A., Bryce D.L.* // Angew. Chem. Int. Ed. – 2012. – **51**. – P. 4227.

27. *Perras F.A., Widdifield C.M., Bryce D.L.* // Solid State Nucl. Magn. Reson. – 2012. – **45-46**. – P. 36.

28. *Fernelius W.C.* Inorganic Synthesis. Vol. II. – N.Y.: McGraw-Hill, 1946.

29. *Milne J.B., Gabe E.J., Bensimon C.* // Can. J. Chem. – 1991. – **69**. – P. 648.

30. *Collins M.J., Ripmeester J.A., Sawyer J.F.* // J. Am. Chem. Soc. – 1987. – **109**. – P. 4113.

31. *Massiot D., Fayon F., Capron M., King I., Le Calvé S., Alonso B., Durand J.-O., Bujoli B., Gan Z., Hoatson G.* // Magn. Reson. Chem. – 2002. – **40**. – P. 70.

32. *Clark S.J., Segall M.D., Pickard C.J., Hasnip P.J., Probert M.J., Refson K., Payne M.C.* // Z. Kristallogr. – 2005. – **220**. – P. 567.

33. *Profeta M., Mauri F., Pickard C.J.* // J. Am. Chem. Soc. – 2003. – **125**. – P. 541.

34. *Pickard C.J., Mauri F.* // Phys. Rev. B. – 2001. – **63**. – P. 245101.

35. *Yates J.R., Pickard C.J., Mauri F.* // Phys. Rev. B. – 2007. – **76**. – P. 024401.

36. *Engel G.* // Z. Kristallogr., Kristallgeom., Kristallphys., Kristallchem. – 1935. – **90**. – P. 341.

37. *Abriel W.* // Acta Crystallogr. C. – 1986. – **42**. – P. 1113.

38. *Hazell A.C.* // Acta Chem. Scand. – 1966. – **20**. – P. 165.

39. *Webster M., Collins P.H.* // J. Chem. Soc., Dalton Trans. – 1973. – P. 588.

40. *Krebs B., Ahlers F.-P.* // Adv. Inorg. Chem. – 1990. – **35**. – P. 235.

41. *Gabuda S.P., Kozlova S.G., Lapina O.B., Terskikh V.V.* // Chem. Phys. Lett. – 1998. – **282**. – P. 245.

42. *Gabuda S.P., Kozlova S.G.* // J. Phys. Chem. B. – 2006. – **110**. – P. 18091.

43. *Gabuda S.P., Kozlova S.G.* // J. Struct. Chem. – 1997. – **38**. – P. 140.

44. *Kozlova S.G., Gabuda S.P., Blinc R.* // Chem. Phys. Lett. – 2003. – **376**. – P. 364.

45. *Nakamura D., Ito K., Kubo M.* // J. Am. Chem. Soc. – 1962. – **84**. – P. 163.

46. *Nakamura D., Ito K., Kubo M.* // Inorg. Chem. – 1963. – **2**. – P. 61.

47. *Chadha R.K., Miller J.M.* // Can. J. Chem. – 1982. – **60**. – P. 2256

48. *Pietikäinen J., Maaninen A., Laitinen R.S., Oilunkaniemi R., Valkonen J.* // Polyhedron. – 2002. – **21**. – P. 1089.

49. *Närhi S.M., Oilunkaniemi R., Laitinen R.S., Ahlgrén M.* // Acta Crystallogr. E. – 2004. – **60**. – P. o798.

50. *Collins M.J., Ripmeester J.A., Sawyer J.F.* // J. Am. Chem. Soc. – 1988. – **110**. – P. 8583.

51. *Hayashi S., Hayamizu K.* // Magn. Reson. Chem. – 1992. – **30**. – P. 658.

52. *Ziolo R.F., Extine M.* // Inorg. Chem. – 1980. – **19**. – P. 2964.

53. *Chopra A., Jain S., Srivastava S.K., Gupta S.K., Butcher R.J.* // Acta Crystallog., Sect. E. – 2014. – **70**. – P. o421.

54. *Oilunkaniemi R., Pietikäinen J., Laitinen R.S., Ahlgrén M.* // J. Organomet. Chem. – 2001. – **640**. – P. 50.